AD-A064 812 UNIVERSITY OF SOUTHERN CALIFORNIA LOS ANGELES DEPT O--ETC F/G 12/1
NON-NORMAL INCIDENCE STATE SPACE MODEL.(U)
1978 F AMINZADEH, J M MENDEL AFOSR-75-2797

UNCLASSIFIED AFOSR-TR-79-0048 NL

1 OF 1
ADA
064812

END
DATE
FILMED
4-79
DDC

Society of Exploration Geophysicists
Box 3098
Tulsa, Oklahoma 74101

Preprint subject to later revision, for information of delegates to the SEG Annual Meeting only.

NON-NORMAL INCIDENCE STATE SPACE MODEL

See back page for 1473

by

Fereydoun Aminzadeh and Jerry M. Mendel
Department of Electrical Engineering
University of Southern California
Los Angeles, California 90007

Discussion of this paper is invited immediately after its presentation. Written discussions will be considered for publication in GEOPHYSICS, should the paper be accepted for publication.

"Non-Normal Incidence State Space Model"

by

F. Aminzadeh and J. M. Mendel
Department of Electrical Engineering
University of Southern California
Los Angeles, California 90007

Abstract

The primary purpose of this paper is to extend a newly published normal incidence state space model [Ref. 1] to the non-normal incidence case. It also provides a synthetic seismogram for a two-dimensional point source and different offsets. The non-normal incidence state space model is structurally the same as the normal incidence state space model except that it has twice as many state variables. Because of the mode conversion in non-normal incidence, the scalar upgoing and downgoing waves and travel times in each layer as well as reflection and transmission coefficients at each interface are replaced by a vector of upgoing and downgoing waves, a vector of travel time, and matrices of reflection and transmission coefficients, respectively. To obtain a two-dimensional point source synthetic seismogram we apply a new version of Sommerfield's theorem, which is generally used to express a three-dimensional point source in terms of a superposition of line sources.

Introduction

Haskell [2] has developed a frequency-domain method to analyze the behavior of layered media for a non-normal incidence (NNI) plane wave that uses a matrix iteration procedure. His result is a synthetic seismogram in the frequency-domain for an impulsive incident wave. This response can then be inverted back into the time-domain. Wuenschel [3] solved this problem directly in the time-domain for the special case of normal incidence. Frasier [4] gave the solution to this problem in the time-domain for the general case of a plane wave.

Taking advantage of strong results behind the already developed techniques in system theory was good motivation for Nahi and Mendel [5] and Mendel [1] to use a state space model (SSM) to generate a synthetic seismogram for the special case of normal incidence. Because of the novelty of their approach we explain it briefly, as follows.

A system of N layered media is depicted in Fig. 1. Each layer is characterized by its one way travel time τ_n and normal incidence reflection coefficient r_n, $(n = 1,2,\ldots N)$. In Fig. 1, $m(t)$ and $y(t)$ denote the input to and output of the system at interface 0. We assume $u_n(t)$ and $d'_n(t)$ denote the upgoing and downgoing waves in the nth layer, respectively, and that waves at the top of a layer occur at present time t. Using ray theory, waveforms $u_n(t+\tau_n)$ and $d'_{n+1}(t)$ (see Fig. 1) can be written as

$$u_n(t+\tau_n) = r_n d'_n(t-\tau_n) + (1-r_n) u_{n+1}(t) \qquad (1)$$

$$d'_{n+1}(t) = (1+r_n) d'_n(t-\tau_n) - r_n u_{n+1}(t) \qquad (2)$$

For $n = 0$ Eq. (1) gives the output equation, since $u_0(t) \triangleq y(t)$ and $d'_0(t) \triangleq m(t)$; i.e.,

$$y(t) = r_0 m(t) + (1-r_0) u_1(t) \qquad (3)$$

Since we assume the basement acts like an energy sink, no energy is returned from it, which means that $u_{N+1}(t) = 0$; hence, Eq. (1) for n = N has the following form

$$u_N(t+\tau_N) = r_N d'_N(t-\tau_N) \tag{4}$$

Assuming $d'_n(t-\tau_n) \triangleq d_n(t)$ in Eqs. (2) and (4), the *complete* SSM for normal incidence (NI) plane waves in a layered earth model has the following form:

$$\begin{aligned}
d_1(t+\tau_1) &= -r_0\, u_1(t) + (1+r_0)\, m(t) \\
u_1(t+\tau_1) &= r_1\, d_1(t) + (1-r_1)\, u_2(t) \\
&\left.\begin{aligned}
d_n(t+\tau_n) &= (1+r_{n-1})\, d_{n-1}(t) - r_{n-1}\, u_n(t) \\
u_n(t+\tau_n) &= r_n\, d_n(t) + (1-r_n)\, u_{n+1}(t)
\end{aligned}\right\} n = 2,3,\ldots N-1 \\
d_N(t+\tau_N) &= (1+r_{N-1})\, d_{N-1}(t) - r_{N-1}\, u_N(t) \\
u_N(t+\tau_N) &= r_N\, d_N(t)
\end{aligned} \tag{5}$$

Equations (5) and (3) give the complete state space representation of a layered earth for a NI plane wave.

These results, obtained for a normal incidence SSM, lead one to see if they can be generalized to the non-normal incidence (NNI) case. In the following section we develop a NNI SSM for a plane wave source, with θ_0 as its incident angle. Some of Frasier's results are used in this development.

A State Space Model for Non-Normal Incidence Plane Waves

Suppose we have a plane wave source with incident angle θ_0 for the same layered earth model we studied in the normal incidence case. At the bottom of the nth layer (Fig. 2) we define

$DP'_n(t)$ as downgoing P waves

$DS'_n(t)$ as downgoing S waves

$UP'_n(t)$ as upgoing P waves

$US'_n(t)$ as upgoing S waves

At the top of the $(n+1)^{st}$ layer we define

$DP_{n+1}(t)$ as downgoing P waves

$DS_{n+1}(t)$ as downgoing S waves

$UP_{n+1}(t)$ as upgoing P waves

$US_{n+1}(t)$ as upgoing S waves

We also define r_n and r'_n as the reflection coefficients from below and above the nth interface and t_n and t'_n as the transmission coefficients from below and above the nth interface. In the sequel, superscripts of p and s on reflection and transmission coefficients denote the type of mode conversion; e.g., $r_n^{ps} = DS_{n+1}/UP_{n+1}\big|_{US_{n+1} = DP'_n = DS'_n = 0}$. From the definitions of r, r', t and t' we write the following equations at the nth interface,

$$DP_{n+1}(t) = r_n^{pp}\, UP_{n+1}(t) + r_n^{sp}\, US_{n+1}(t) + t_n^{'pp}\, DP_n'(t) + t_n^{'sp}\, DS_n'(t) \qquad (6a)$$

$$DS_{n+1}(t) = r_n^{ps}\, UP_{n+1}(t) + r_n^{ss}\, US_{n+1}(t) + t_n^{'ps}\, DP_n'(t) + t_n^{'ss}\, DS_n'(t) \qquad (6b)$$

$$UP_n'(t) = r_n^{'pp}\, DP_n'(t) + r_n^{'sp}\, DS_n'(t) + t_n^{pp}\, DP_{n+1}(t) + t_n^{sp}\, DS_{n+1}(t) \qquad (6c)$$

$$US_n'(t) = r_n^{'ps}\, DP_n'(t) + r_n^{'ss}\, DS_n'(t) + t_n^{ps}\, DP_{n+1}(t) + t_n^{ss}\, DS_{n+1}(t) \qquad (6d)$$

If the travel time of the P and S waves in the nth layer are assumed to be τ_n^P and τ_n^S, respectively, then the following relations exist between primed and unprimed variables (see Fig. 2):

$$DP_n'(t) = DP_n(t-\tau_n^p) \tag{7a}$$

$$DS_n'(t) = DS_n(t-\tau_n^s) \tag{7b}$$

$$UP_n'(t) = UP_n(t+\tau_n^p) \tag{7c}$$

$$US_n'(t) = US_n(t+\tau_n^s) \tag{7d}$$

Substituting Eq. (7) into Eq. (6) we obtain

$$\begin{aligned}
DP_{n+1}(t) &= r_n^{pp}\, UP_{n+1}(t) + r_n^{sp}\, US_{n+1}(t) + t_n^{'pp}\, DP_n(t-\tau_n^p) + t_n^{'sp}\, DS_n(t-\tau_n^s) \\
DS_{n+1}(t) &= r_n^{ps}\, UP_{n+1}(t) + r_n^{ss}\, US_{n+1}(t) + t_n^{'ps}\, DP_n(t-\tau_n^p) + t_n^{'ss}\, DS_n(t-\tau_n^s) \\
UP_n(t+\tau_n^p) &= r_n^{'pp}\, DP_n(t+\tau_n^p) + r_n^{'sp}\, DS_n(t+\tau_n^s) + t_n^{pp}\, UP_{n+1}(t) + t_n^{sp}\, US_{n+1}(t) \\
US_n(t+\tau_n^s) &= r_n^{'ps}\, DP_n(t+\tau_n^p) + r_n^{'ss}\, DS_n(t+\tau_n^s) + t_n^{ps}\, UP_{n+1}(t) + t_n^{ss}\, US_{n+1}(t)
\end{aligned} \tag{8}$$

If we define the following notations

$$\underline{D}_n(t) \triangleq \begin{bmatrix} DP_n(t) \\ DS_n(t) \end{bmatrix} \tag{8a}$$

$$\underline{U}_n(t) \triangleq \begin{bmatrix} UP_n(t) \\ US_n(t) \end{bmatrix} \tag{8b}$$

$$\underline{\tau}_n \triangleq \begin{bmatrix} \tau_n^p \\ \tau_n^s \end{bmatrix} \tag{8c}$$

$$\underline{D}_n(t-\underline{\tau}_n) \triangleq \begin{bmatrix} DP_n(t-\tau_n^p) \\ DS_n(t-\tau_n^s) \end{bmatrix} \tag{8d}$$

$$\underline{U}_n(t-\underline{\tau}_n) \triangleq \begin{bmatrix} UP_n(t-\tau_n^p) \\ US_n(t-\tau_n^s) \end{bmatrix} \tag{8e}$$

$$\mathbf{R}_n = \begin{bmatrix} r_n^{pp} & r_n^{sp} \\ r_n^{ps} & r_n^{ss} \end{bmatrix} \tag{8f}$$

$$\mathbf{R}_n' = \begin{bmatrix} r_n'^{pp} & r_n'^{sp} \\ r_n'^{ps} & r_n'^{ss} \end{bmatrix} \tag{8g}$$

$$\mathbf{T}_n = \begin{bmatrix} t_n^{pp} & t_n^{sp} \\ t_n^{ps} & t_n^{ss} \end{bmatrix} \tag{8h}$$

and

$$\mathbf{T}_n' = \begin{bmatrix} t_n'^{pp} & t_n'^{sp} \\ t_n'^{ps} & t_n'^{ss} \end{bmatrix} , \tag{8i}$$

then Eq. (8) can be written in the following vector form:

$$\underline{D}_{n+1}(t) = R_n \underline{U}_{n+1}(t) + T_n' \underline{D}_n(t-\underline{\tau}_n) \tag{9a}$$

$$\underline{U}_n(t+\underline{\tau}_n) = R_n' \underline{D}_n(t-\underline{\tau}_n) + T_n \underline{U}_{n+1}(t) \tag{9b}$$

If we apply the following change of variables to Eq. (9)

$$\underline{d}_n(t) \triangleq \underline{D}_n(t-\underline{\tau}_n) \tag{10a}$$

$$\underline{u}_n(t) \triangleq \underline{U}_n(t) , \tag{10b}$$

and write Eq. (9a) for $n \Rightarrow n-1$, then we obtain

$$\underline{d}_n(t+\underline{\tau}_n) = R_{n-1} \underline{u}_n(t) + T_{n-1}' \underline{d}_{n-1}(t) \tag{11a}$$

$$\underline{u}_n(t+\underline{\tau}_n) = R_n' \underline{d}_n(t) + T_n \underline{u}_{n+1}(t) \tag{11b}$$

Equation (11) is valid for n = 2,3, ...N-1. For n = 1, Eq. (11b) is still valid, while in Eq. (11a), $d_0(t) = d_{n-1}(t)\Big|_{n=1}$ should be replaced by $\underline{m}(t)$, the input vector. For n = N, Eq. (11a) doesn't change, but in Eq. (11b), the $T_N\,\underline{u}_{N+1}(t)$ term should be eliminated, since we assume there is no return from below the Nth interface (basement). These considerations lead to the following <u>state space equations</u> for a <u>NNI plane wave source</u>.

$$
\begin{aligned}
\underline{d}_1(t+\underline{\tau}_1) &= R_0\,\underline{u}_1(t) + T_0'\,\underline{m}(t)\\
\underline{u}_1(t+\underline{\tau}_1) &= R_1'\,\underline{d}_1(t) + T_1\,\underline{u}_2(t)\\
\left.\begin{aligned}
\underline{d}_n(t+\underline{\tau}_n) &= T_{n-1}'\,\underline{d}_{n-1}(t) + R_{n-1}\,\underline{u}_n(t)\\
\underline{u}_n(t+\underline{\tau}_n) &= R_n'\,\underline{d}_n(t) + T_n\,\underline{u}_{n+1}(t)
\end{aligned}\right\}& \quad n = 2,3,\ \ldots N-1\\
\underline{d}_N(t+\underline{\tau}_N) &= T_{N-1}'\,\underline{d}_{N-1}(t) + R_{N-1}\,\underline{u}_N(t)\\
\underline{U}_N(t+\underline{\tau}_N) &= R_N'\,\underline{d}_N(t)
\end{aligned}
\tag{12}
$$

The output equation is given by

$$\underline{y}(t) = T_0\,\underline{u}_1(t) + R_0'\,\underline{m}(t) \tag{13}$$

where

$$\underline{y}(t) \ \underline{\Delta} \begin{bmatrix} y^p(t) \\ y^s(t) \end{bmatrix} \tag{14}$$

and $y^p(t)$ and $y^s(t)$ denote the particle velocity. In Eq. (14) $y^p(t)$ and $y^s(t)$ denote the particle velocity on the top of zeroth interface for P and S waves. These particle velocities for P and S waves are measured in the direction of P and S vectors and result from P and S wave potentials, respectively. The seismogram equations in z and x direction are given by

$$y^z_{total} = [\cos\theta_0, \sin\phi_0]\,\underline{y}(t) = \cos\theta_0\, y^P(t) + \sin\phi_0\, y^s(t) \tag{15a}$$

and

$$y^x_{total} = [\sin\theta_0, -\cos\phi_0]\,\underline{y}(t) = \sin\theta_0\, y^P(t) - \cos\phi_0\, y^s(t) \tag{15b}$$

where θ_0 and ϕ_0 are P and S wave angles with the normal on the top of the zeroth interface.

Equations (12) and (15) are the complete NNI, SSM and measurement equations, and are similar to Eqs. (5) and (3) for the normal incidence case.

If we assume that

$$\underline{x} \triangleq [d_1^p, d_1^s, u_1^p, u_1^s, \ldots d_N^p, d_N^s, u_N^p, u_N^s]^t \tag{16}$$

$$Z_i \triangleq \text{diag}[z_i^p, z_i^s] \quad , \quad i = 1,2,\ldots N \tag{17}$$

and

$$Z \triangleq \text{diag}[Z_1, Z_1, Z_2, Z_2, \ldots Z_N, Z_N] \, , \tag{18}$$

where z_i^p and z_i^s are delay operators, defined by

$$\left.\begin{aligned} z_i^p\, f(t) &= f(t-\tau_i^p) \\ z_i^s\, f(t) &= f(t-\tau_i^s) \end{aligned}\right\} \quad i = 1,2, \ldots N \, , \tag{19}$$

then Eqs. (12) and (15) can be written as

$$Z^{-1}\, \underline{x}(t) = A\, \underline{x}(t) + \underline{b}\, m^p(t) \tag{20}$$

$$y^z_{total} = \underline{c}\, \underline{x}(t) + d\, m^p(t) \tag{21}$$

In Eqs. (20) and (21) we have assumed the input source to be of the form

$$\underline{m}(t) = \begin{bmatrix} m^p(t) \\ 0 \end{bmatrix} \tag{22}$$

This is in accordance with practical experiments which use a compressional source.

The explicit forms of A, $\underline{b}$, $\underline{c}$ and d for a special case of a two-layer earth model are given in the following example.

<u>Example</u>: The NNI, SSM for a two-layer model is:

$$d_1^p(t+\tau_1^p) = r_0^{pp}\, u_1^p(t) + r_0^{sp}\, u_1^s(t) + t_0^{'pp}\, m^p(t)$$

$$d_1^s(t+\tau_1^s) = r_0^{ps}\, u_1^p(t) + r_0^{ss}\, u_1^s(t) + t_0^{'ps}\, m^p(t)$$

$$
\begin{aligned}
u_1^p(t+\tau_1^p) &= t_2^{pp}\, u_2^p(t) + t_2^{sp}\, u_2^s(t) + r_1^{'pp}\, d_1^p(t) + r_1^{'sp}\, d_1^s(t) \\
u_1^s(t+\tau_1^s) &= t_2^{ps}\, u_2^p(t) + t_2^{ss}\, u_2^s(t) + r_1^{'ps}\, d_1^p(t) + r_1^{'ss}\, d_1^s(t) \\
d_2^p(t+\tau_2^p) &= r_1^{pp}\, u_2^p(t) + r_1^{sp}\, u_2^s(t) + t_1^{'pp}\, d_1^p(t) + t_1^{'sp}\, d_1^s(t) \\
d_2^s(t+\tau_2^s) &= r_1^{ps}\, u_2^p(t)\; r_1^{ss}\, u_2^s(t) + t_1^{'ps}\, d_1^p(t) + t_1^{'ss}\, d_1^s(t) \\
u_2^p(t+\tau_2^p) &= r_2^{'pp}\, d_2^p(t) + r_2^{'sp}\, d_2^s(t) \\
u_1^s(t+\tau_2^s) &= r_2^{'ps}\, d_2^p(t) + r_2^{'ss}\, d_2^s(t)
\end{aligned}
\tag{23}
$$

The measurement equation is given by

$$
\begin{aligned}
y^z_{total}(t) = {} & (t_0^{pp} \cos\theta_0 + t_0^{sp} \sin\phi_0)\, u_1^p(t) + \\
& (t_0^{ps} \cos\theta_0 + t_0^{ss} \sin\phi_0)\, u_1^s(t) + \\
& (r_0^{'pp} \cos\theta_0 + r_0^{'sp} \sin\phi_0)\, m^P(t)
\end{aligned}
\tag{24}
$$

Using definitions given by Eqs. (16), (17) and (18), Eqs. (23) and (24) can be written as in Eqs. (20) and (21) with A, $\underline{b}$, $\underline{c}$ and d given by

$$
A = \left[\begin{array}{cc|cc|cc|cc}
0 & 0 & r_0^{pp} & r_0^{sp} & 0 & 0 & 0 & 0 \\
0 & 0 & r_0^{ps} & r_0^{ss} & 0 & 0 & 0 & 0 \\
\hline
r_1^{'pp} & r_1^{'sp} & 0 & 0 & 0 & 0 & t_2^{pp} & t_2^{sp} \\
r_1^{'ps} & r_1^{'ss} & 0 & 0 & 0 & 0 & t_2^{ps} & t_2^{ss} \\
\hline
t_1^{'pp} & t_1^{'sp} & 0 & 0 & 0 & 0 & r_1^{pp} & r_1^{sp} \\
t_1^{'ps} & t_1^{'ss} & 0 & 0 & 0 & 0 & r_1^{ps} & r_1^{ss} \\
\hline
0 & 0 & 0 & 0 & r_2^{'pp} & r_2^{'sp} & 0 & 0 \\
0 & 0 & 0 & 0 & r_2^{'ps} & r_2^{'ss} & 0 & 0
\end{array}\right]
\tag{25}
$$

$$\underline{b} = \left[t_0'^{pp} \quad t_0'^{sp} \;\middle|\; 0 \quad 0 \;\middle|\; 0 \quad 0 \;\middle|\; 0 \quad 0 \right]$$

$$\underline{c} = \left[0 \quad 0 \;\middle|\; t_0^{pp} \cos\theta_0 + t_0^{sp} \sin\phi_0,\ t_0^{ps} \cos\theta_0 + t_0^{ss} \sin\phi_0 \;\middle|\; 0 \quad 0 \;\middle|\; 0 \quad 0 \right] \tag{27}$$

and

$$d = r_0'^{pp} \cos\theta_0 + r_0'^{sp} \sin\phi_0 \tag{28}$$

Evaluation of System Parameters

In this section we evaluate the parameters of the system given by Eqs. (12) and (15). The travel times of P and S waves in different layers are a function of θ_i and ϕ_i, $i = 1,2,\ldots N$ which are the angles of direction of propagation of P and S waves with respect to the normal in different layers. This is because of the fact that, in the plane wave case, for each layer there is unique angles associated with P and S waves. Given the incident angle of the plane wave source, θ_0, the angles θ_n and ϕ_n are uniquely determined by Snell's law, using the velocity information of the subsurface. Knowing θ_n, ϕ_n and h_n, v_n^p and v_n^s (the thickness and the P and S wave velocities of the nth layers, respectively), we calculate $\underline{\tau_n}$, $n = 1,2,\ldots N$, defined by Eq. (8c), from

$$\tau_n^p = h_n \cos\theta_n / v_n^p \tag{29}$$

$$\tau_n^s = h_n \cos\phi_n / v_n^s \tag{30}$$

The τ_n^p and τ_n^s are the travel times in nth layer for P and S waves assuming that the measurement is made at $n = 0$. For example, τ_1^p is half of the time in which path OFE_1 of Fig. 3 is traveled. From Fig. 3 it is straightforward to show that τ_1^p satisfies Eq. (29). ($\tau_1^p = \frac{1}{2}\,\frac{OF + FE_1}{v_1^p} = \frac{OF + OF\cdot\cos 2\theta_1}{2 v_1^p} = \frac{h}{2 v_1^s \cos\theta_1}(1 + \cos 2\theta_1) = \frac{h}{v_1^p}\cos\theta_1$). The proof of Eq. (29) for $i > 1$ and the proof of Eq. (30) is similar. For measurements made at $x = 0$, we can obtain the actual seismogram at $x = x_1$ by using the following property of plane waves; (shifting property):

<u>Shifting property</u>: For an incident plane wave, relocating the sensors by an amount x, affects the received signal by a phase shift of x_1/C_{θ_0} where C_{θ_0} is the phase velocity and is a function of the incident angle of the source, θ_0.

<u>Proof</u>: We just showed that if we make the measurement at $x = 0$ (at 0 in Fig. 3) then the travel time is the time in which the distance of OFE_1 is traveled. On the other hand, if the measurement is made at a nonzero offset, say at E, then from Fig. 3, an extra distance, EE_1 should be traveled. For a P wave this takes τ_{delay} seconds, where

$$\tau_{delay} = EE_1/v_1^p \tag{31}$$

From geometry we have

$$EE_1 = OE \sin \theta_1 \quad .$$

Substituting this expression into Eq. (31), we obtain

$$\tau_{delay} = OE/(v_1^p/\sin \theta_1) \quad .$$

From Snell's law, $v_1^p/\sin \theta_1$ is the phase velocity and is a function of incident angle θ_0 ($C_{\theta_0} = \frac{v_0^p}{\sin \theta_0}$). Assuming $OE = x_1$, we obtain

$$\tau_{delay} = x_1/C_{\theta_0} \tag{32}$$

which concludes the proof.

The computation of A, $\underline{b}$, $\underline{c}$ and d requires knowledge of R_n, T_n, R'_n and T'_n for $n = 0,1,\ldots N$. Although the continuity equations of particle velocity and stress, ($\frac{\dot{u}}{c}$, $\frac{\dot{w}}{c}$, τ_{zz}, τ_{zx}), are the usual tools used to compute the reflection and transmission coefficient matrices, they require the inversion of 4×4 matrices, which is not desirable. Frasier [4] has developed the following relations to compute T'_n and R'_n; they only require the inversion of 2 × 2 matrices

$$T'_n = 2 L_{n+1} (B_n^{-1} B_{n+1} + A_n^{-1} A_{n+1})^{-1} L_n^{-1} \tag{33}$$

$$R'_n = \frac{1}{2} L_n (B_n^{-1} (B_n^{-1} B_{n+1} - A_n^{-1} A_{n+1})^{-1} L_{n+1}^{-1} T'_n \tag{34}$$

where

$$L_n = \begin{bmatrix} \sqrt{\rho_n q_n^p} & 0 \\ 0 & \sqrt{\rho_n q_n^s} \end{bmatrix} \tag{35}$$

$$A_n = \begin{bmatrix} -q_n^p & 1 \\ 2 \rho_n (\frac{v_n^s}{c})^2 q_n^p & \rho_n \gamma_n \end{bmatrix} \tag{36}$$

$$B_n = \begin{bmatrix} -1 & q_n^s \\ -\rho_n \gamma_n & 2 \rho_n (\frac{v_n^s}{c})^2 q_n^s \end{bmatrix} \tag{37}$$

$$q_n^p = \sqrt{(\frac{c}{v_n^p})^2 - 1} \tag{38}$$

$$q_n^s = \sqrt{(\frac{c}{v_n^s})^2 - 1} \tag{39}$$

$$\gamma_n = 1 - 2(\frac{v_n^s}{c})^2 \tag{40}$$

for n = 0,1,2,...N. In these equations, ρ_n is the density of the nth layer and c stands for C_{θ_0}. To compute R_n and T_n we can interchange the indices of n and n+1 in the right-hand side of Eqs. (33) and (34). We can also use the following relations given by Frasier [4].

$$T_n = T_n'^T \tag{41}$$

$$R_n = -T_n^{-1} R_n' T_n \tag{42}$$

Using Snell's law ($\frac{v_n^s}{c} = \sin\phi_n$ and $\frac{v_n^p}{c} = \sin\theta_n$), we express q_n^p, q_n^s and γ_n, ($n = 0,1,2,\ldots N$) in terms of θ_i and ϕ_i, and ρ_i, $i = 1,2,\ldots N$, as

$$q_n^p = \operatorname{cotg}\theta_n \tag{43}$$

$$q_n^s = \operatorname{cotg}\phi_n \tag{44}$$

and

$$\gamma_n = \cos 2\phi_n \tag{45}$$

Substituting q_n^p, q_n^s and γ_n from Eqs. (43), (44) and (45), into Eqs. (35), (36) and (37), we obtain

$$L_n = \begin{bmatrix} \sqrt{\rho_n \operatorname{cotg}\theta_n} & 0 \\ 0 & \sqrt{\rho_n \operatorname{cotg}\phi_n} \end{bmatrix} \tag{46}$$

$$A_n = \begin{bmatrix} -\operatorname{cotg}\theta_n & 1 \\ 2\rho_n \sin^2\phi_n \operatorname{cotg}\theta_n & \rho_n \cos 2\phi_n \end{bmatrix} \tag{47}$$

$$B_n = \begin{bmatrix} -1 & -\operatorname{cotg}\phi_n \\ -\rho_n \cos 2\phi_n & \rho_n \sin 2\phi_n \end{bmatrix} \tag{48}$$

It is interesting to note that, in the case of normal incidence, these expressions reduce to well-known normal incidence relationships:

$$r_n^{ps} = r_n^{sp} = r_n'^{ps} = r_n'^{sp} = t_n^{ps} = t_n^{sp} = t_n'^{ps} = t_n'^{sp} = 0 \tag{49}$$

Derivation of a 2-D Point Source Seismogram

In the previous section we developed a NNI seismogram for a plane wave source with an incident angle θ_0. Although a plane wave source physically can be approximated by a group of point sources, an exact plane wave source doesn't exist. Most of the sources used in exploration geophysics are point sources. Consequently plane wave source techniques are not suitable for practical problems and are mostly of a theoretical value.

As the first step towards obtaining a more realistic seismogram, we introduce the idea of 2-D point source. The derivation of a 3-D point source seismogram from a 2-D point source seismogram remains to be studied.

In this section we obtain a two-dimensional point source seismogram from our NNI plane wave seismogram. A complete algorithm for obtaining our 2-D point source synthetic seismogram is given at the end of this section.

To obtain the 2-D point source synthetic seismogram, we use a theorem similar to one which is given by Sommerfield [Ref. 6] which expresses a point source as a superposition of line sources.

<u>Theorem 1</u>: A cylinderical line source can be considered as the superposition of plane waves, whose incident angles range from $-\frac{\pi}{2}$ to $\frac{\pi}{2}$, and refractive waves which can be thought of as plane waves with complex incident angles.

Before proving this theorem we present three different representations of a wave for a pressure field, the first in spherical coordinates, the second in cylinderical coordinates and the third in cartesian coordinates:

$$\psi_1(t,R) = \frac{e^{-ik_\alpha R}}{R} e^{i\omega t} \tag{50}$$

$$\psi_2(t,z,r) = J_0(k_\alpha r)\, e^{-\nu|z|}\, e^{i\omega t} \tag{51}$$

$$\psi_3(t,x,y,z) = e^{ik(ct-x-ay-bz)} \tag{52}$$

Ewing et al [6] have shown that $\psi_1(t,R)$ given by Eq. (50) can be expressed in terms of $\psi_2(t,z,r)$ given by Eq. (51), using weighted travel times; i.e.

$$\frac{1}{R} e^{-ik_\alpha R} = \int_0^\infty J_0(kr)\, e^{-\nu|z|}\, F(k)\, dk \tag{53}$$

where

$$F(k) = \frac{k}{\sqrt{k^2 - k_\alpha^2}} = \frac{k}{\nu} \tag{54}$$

Theorem 1 demonstrates the possibilities of relating $\psi_2(t,r,z)$ to $\psi_3(t,x,y,z)$, through a superposition relationship.

<u>Proof of Theorem 1</u>: We start with the following representation of a cylinderical wave-front

$$\psi_0(r,t) = H_0^2(k_\alpha r)\, e^{ikct} \tag{55}$$

where $H_0^2(k_\alpha r)$ is a Hankel function of the second kind that is related to Bessel functions of the first and second kind. (To see the relationship refer to [8].)

The time-varying part of Eq. (55) appears in the plane wave representation too, so we exclude that term in our derivation, and show that

$$H_0^2(k_\alpha r) = \frac{1}{\pi}\int_{-\frac{\pi}{2}}^{\frac{\pi}{2}} \exp\,[ik_\alpha(-x \sin\theta - z\cos\theta)]\, d\theta$$

$$+ \left[\frac{2i}{\pi}\int_{k_\alpha}^{\infty} e^{-\nu z - ikx}\,\frac{dk}{\nu}\right] \tag{56}$$

The first term in the r.h.s. of Eq. (56) represents a sum of plane waves with incident angles which range from $-\frac{\pi}{2}$ to $\frac{\pi}{2}$ (the reflection terms), while the second term can be considered due to so-called non-real incident-angle plane waves with real ν, which are attenuated as z increases (refracted waves).

According to [Ref. 7], from the definition of Hankel function, we can write $H_0^2(k_\alpha r)$ in the following form

$$H_0^2(k_\alpha r) = -\frac{2}{i\pi}\int_0^\infty e^{-\nu|z|}\cos kx\,\frac{dk}{\nu} \tag{57}$$

For $z > 0$ we have

$$\begin{aligned}
H_0^2(k_\alpha r) &= -\frac{2}{i\pi}\int_0^\infty e^{-\nu z}\cos kx\,\frac{dk}{\nu} \\
&= -\frac{2}{i\pi}\int_0^{k} e^{-\nu z}\cos kx\,\frac{dk}{\nu} + \frac{2i}{\pi}\int_{k_\alpha}^\infty e^{-\nu z}\cos kx\,\frac{dk}{\nu} \\
&= -\frac{1}{i\pi}\int_{-k_\alpha}^{k_\alpha} e^{-\nu z - ikx}\,\frac{dk}{\nu} + \frac{2i}{\pi}\int_{k_\alpha}^\infty e^{-\nu z}\cos kx\,\frac{dk}{\nu} \\
&= \frac{1}{\pi}\int_{-\frac{\pi}{2}}^{\frac{\pi}{2}} e^{-ik_\alpha(-X\sin\theta - z\cos\theta)}\,d\theta + \frac{2i}{\pi}\int_{k_\alpha}^\infty e^{-\nu z}\cos kX\,\frac{dk}{\nu}
\end{aligned}$$

where we have made use of the fact that $k = k_\alpha \sin\theta$ and $\nu^2 = k^2 - k_\alpha^2$. This completes the proof of theorem 1.

Our seismogram consists only of the first term of Eq. (56) and so it is called a <u>2-D point source reflection synthetic seismogram (2D-PSRSS)</u>. The term in brackets in Eq. (56) is the refractional component because it is due to so-called complex incident angles. These waves are known as inhomogeneous plane waves.

Next we summarize the algorithm used to obtain a two-dimensional point source reflection synthetic seismogram (2D-PSRSS) from a NNI plane wave seismogram. Figure 4 shows the different steps of the following algorithm.

<u>Step 1</u>: (Initialization): Set $j = 1$ and $\theta_j = -\frac{\pi}{2}$ and $\sum_i = 0$, $i = 1,2,\ldots K$. θ_j is the incident angle of the plane wave source and $\sum_i$ is the 2D-PSRSS in the

final step for offset $x = x_i$; K is the total number of traces.

Step 2: Obtain a NNI plane wave seismogram for θ_j, measured at $n = 0$. Call this seismogram $F(t,\theta_j,0)$. Set $k = 1$.

Step 3: Use the shifting property to obtain the output $F(t,\theta_j,n_k)$ at $x = x_k$. Set $\sum_k = \sum_k + F(t,\theta_j,x_k)$.

Step 4: Set $k = k+1$. If k is less than or equal to K go to step 3.

Step 5: Set $j = j+1$ and $\theta_j = \theta_{j-1} + \Delta\theta$ ($\Delta\theta$ is an angle increment chosen a priori). If θ_j is less than $\frac{\pi}{2}$ go to step 1.

Step 6: Set $J = j-1$, divide $\sum_k$ by J, $k = 1,2,\ldots K$.

When we reach step 6 we have K traces each one of which is the 2D-PSRSS for offsets $x = x_k$, $k = 1, 2, \ldots K$.

Note. Because of the given structure of the subsurface we might reach the critical angle $\hat{\theta}$ for $|\theta| < \frac{\pi}{2}$. In that case we have to modify our algorithm to exclude any possible imaginary angle in some layers.

Simulation Results

We have used our algorithm to obtain a NNI plane wave seismogram and a 2-D point source reflection seismogram for an acoustic medium as well as an elastic medium. The simulation results for acoustic and elastic cases are for models with specifications given in Tables 1 and 2, respectively.

Figures 5 and 6 are the NNI plane wave seismograms for incident angles $0.,2.5,\ldots,22.5^\circ$ for acoustic and elastic media, respectively. We notice that the plane wave seismogram for the acoustic case is identical for different incident angles except for a change in arrival times (the variation of reflection coefficients is not considerable). In the elastic case as we increase the incident angle some new reflections which are due to mode conversion appear in the seismogram. The NNI plane wave seismogram in the x direction, for the elastic case, is shown in Figure 7. We also notice that for zero incident angle the results of acoustic and elastic cases in the z direction (the first trace in Figures 5 and 6) are identical. Also the x direction component of elastic model for NI is identically zero.

We have also generated 2-D point source synthetic seismograms for both acoustic and elastic models. The measurements are assumed to be at x = 0, 100, ..., 800 ft. Figures 8 and 9 are the results of the simulation for a 2- and 3-layer acoustic model. As we notice from Figures 8 and 9 the set of peaks of each arrival (primary or multiple) has a hyperbolic form in the x-z plane. The exponential decay for each arrival is in accordance with the results given by Dampney [10] for a 2-D point source.

Figures 10 and 11 are the results of simulation for a 2-layer elastic model in z- and x-directions, respectively. The hyperbolic characteristics of peaks in the x-z plane is still recognizable. If the travel times of P and S waves were not too close we could have seen hyperbolas with different concavity for P and S waves, more clearly.

Table 1 The specification of the acoustic model used in our simulations

layer number	velocity (ft/sec)	density gm/cm^3	NI travel time (sec)
0	10000	12	-
1	2000	3	0.14
2	1900	2.4	0.26
3	1200	2.1	0.18
4	1700	2.7	-

Table 2 The specification of the elastic model used in our simulation

layer number	P wave velocity ft/sec	S wave velocity ft/sec	density gm/cm^3	NI travel time sec
0	10000	9000	12	----
1	2000	1700	3	0.14
2	1900	1600	2.4	0.26
3	1200	1000	2.1	0.18
4	1700	1400	2.7	----

Conclusions

In this paper we have presented a state space approach for obtaining a NNI plane wave synthetic seismogram. This method compared to Haskell's frequency-domain [2] approach and Frasier's transfer function approach [4] has more potential flexibility in applying new seismic data processing techniques such as Kalman filtering and optimal smoothing [Ref. 8], Bremmer series decomposition [Ref. 1] and multiple suppression [Ref. 9]. Furthermore, our NNI synthetic seismogram is in a suitable form to derive the 2-D point source synthetic seismogram.

Our 2-D point source synthetic seismogram, to the best of our knowledge, is an original one.

We have applied the idea of Bremmer series decomposition [Ref. 1] to our NNI plane wave as well as our 2-D point source seismogram. These results as well as suppression of multiples for a NNI plane wave synthetic seismogram are the subject of another paper.

We are also planning to use some parameter estimation techniques to estimate the parameters of the system by minimizing the square of the difference between the output of the two-dimensional point source reflection synthetic seismogram and the output of a seismogram which is obtained using estimated parameters. We will also use the synthetic seismogram obtained by our algorithm for the design of a new multichannel optimal smoother, the general case of the one given by Mendel and Kormylo [Ref. 8]. The output of such a multichannel smoother is a set of deconvolved, noise free estimates of the reflectivity sequence for different offsets. Other seismic data processing techniques such as, stacking, NMO correction, multiple suppression and velocity estimation can be applied to the output of the multichannel optimal smoother. The results of this study will also be the subject of a future paper.

ACKNOWLEDGEMENT

The work reported on in this paper was performed at the University of Southern California, Los Angeles, California, under National Science Foundation Grant NSF ENG 74-02297 A01, Air Force Office of Scientific Research Grant AFOSR 75-2797, Chevron Oil Field Research Co. Contract-76, and U. S. Geological Survey, Department of the Interior, under USGS Grant No. 14-08-0001-G-553.

References

1. J.M. Mendel, "Bremmer Series Decomposition of Solution to the Lossless Wave Equation in Layered Media," IEEE Trans. On GeoScience Electronics, Special Issue on Seismic Data Processing, April 1978.

2. N.A. Haskell, "The Dispersion of Surface Waves on Multilayered Media," Bul. SSA, Vol. 43, pp. 17-34, 1953.

3. P.C. Wuenschel, "Seismogram Synthesis Including Multiples and Transmission Coefficients," Geophysics, Vol. XXV, Feb. 1960, pp. 106-129.

4. C.W. Frasier, "Discrete-Time Solution of Plane P-SV Waves in a Plane Layered Medium," Geophysics, Vol. 35, pp. 197-214, 1970.

5. N.E. Nahi and J.M. Mendel, "A Time-Domain Approach to Seismogram Synthesis for Layered Media," presented at the 46th Annual International Meeting of the SEG, Houston, Texas, Oct. 24-28, 1976.

6. M. Ewing, W.S. Jardetzky and F. Press, "Elastic Waves in Layered Media," McGraw-Hill, New York, 1957.

7. G.N. Watson, "A Treatise on the Theory of Bessel Functions," 2nd. ed. Cambridge Univ. Press, London 1952.

8. J.M. Mendel and J. Kormylo, "Single Channel White Noise Estimator for Deconvolution," Geophysics, Vol. 34, No. 1, Feb. 1978.

9. J.S. Lee and J.M. Mendel, "Supression of Multiples," unpublished.

10. C.N.G. Dampney, "The Relationship Between Two and Three Dimensional Elastic Wave Propagation," Bulletin of Seismological Society of America, Vol. 61, No. 6, pp. 1583-1588, Dec. 1971.

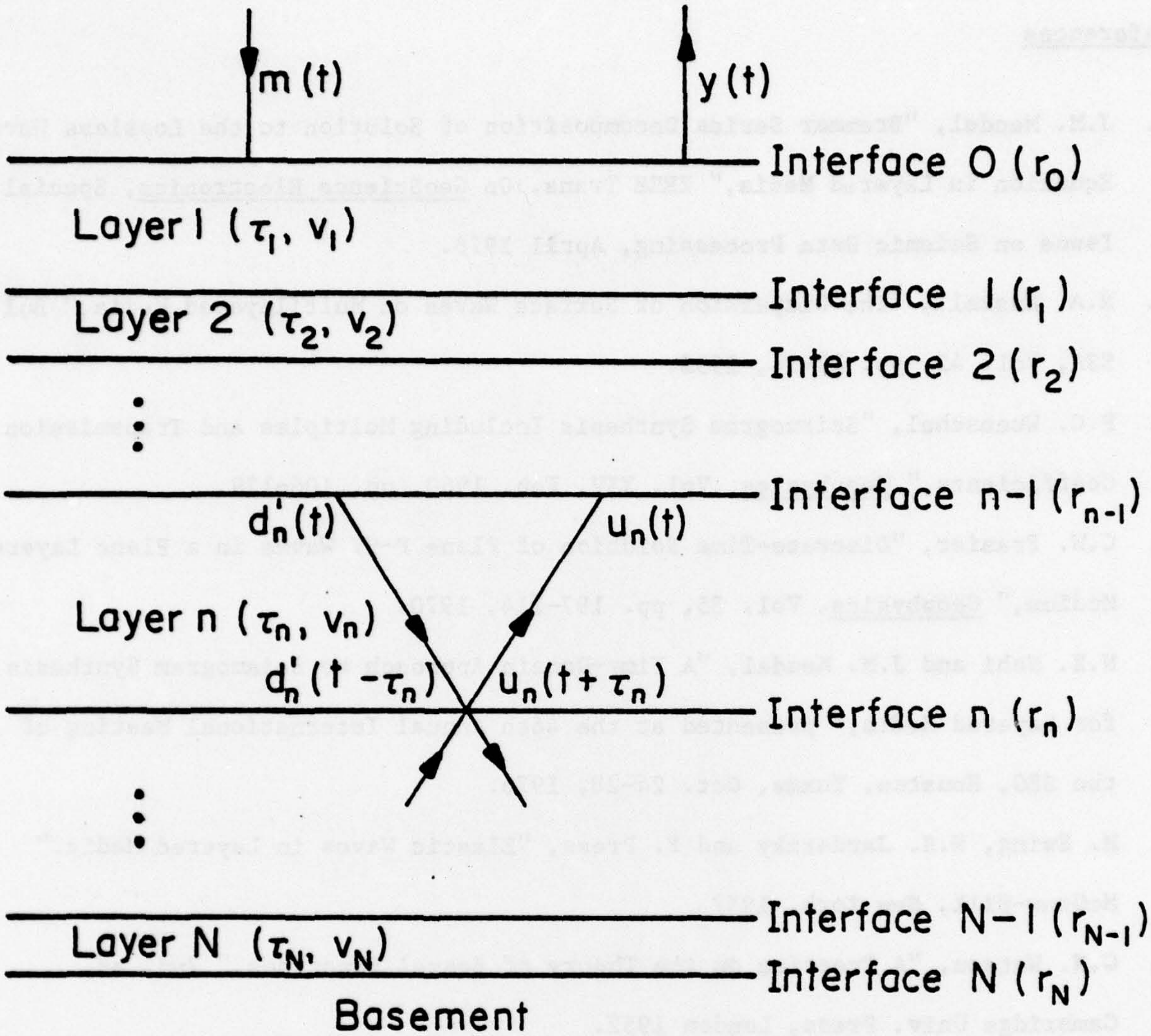

FIG. 1 System of N Layered Media with reflected and transmitted waves at interface n

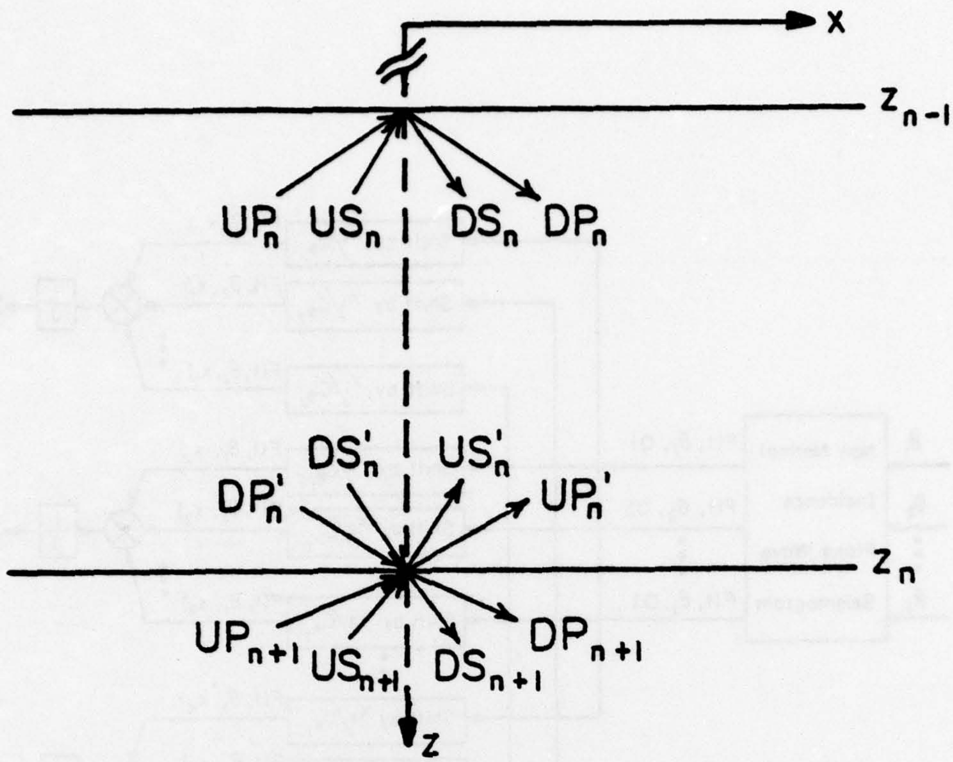

FIG. 2 A representation of upgoing and downgoing P and S waves at n^{th} interface

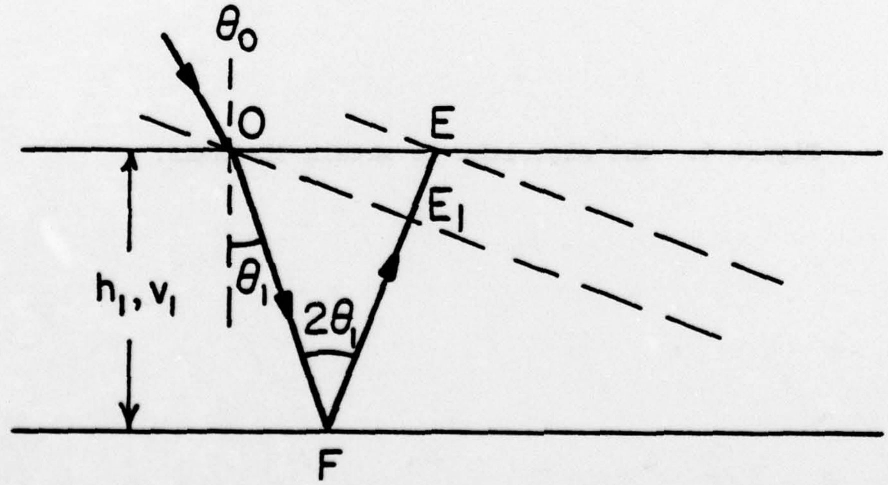

FIG. 3 Wavefronts at a frozen instant of time

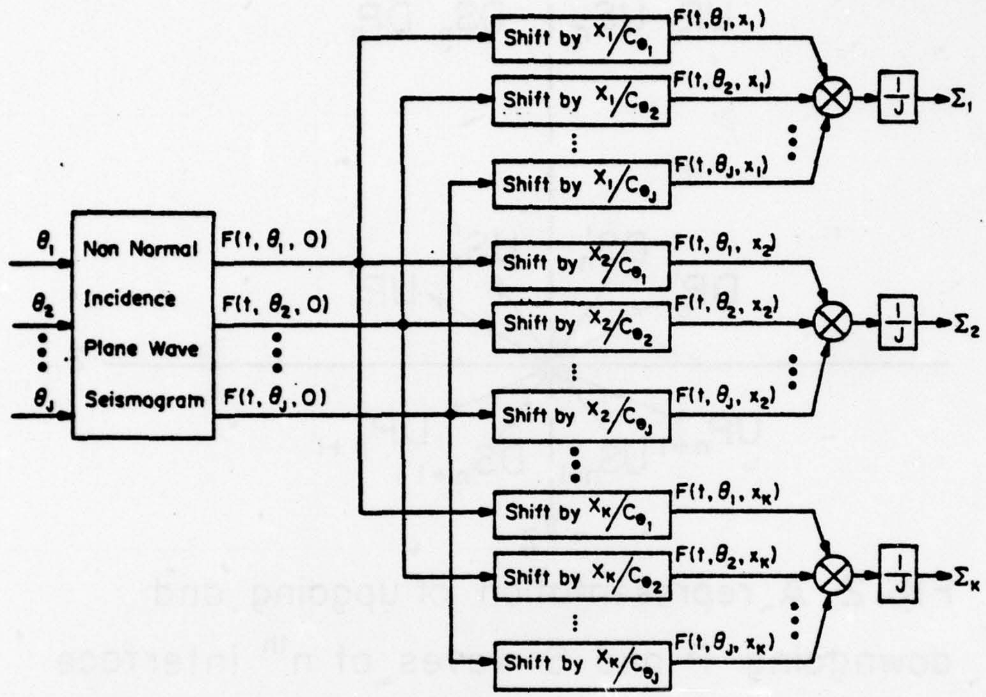

Figure 4. The algorithm to obtain 2D-PSRSS.

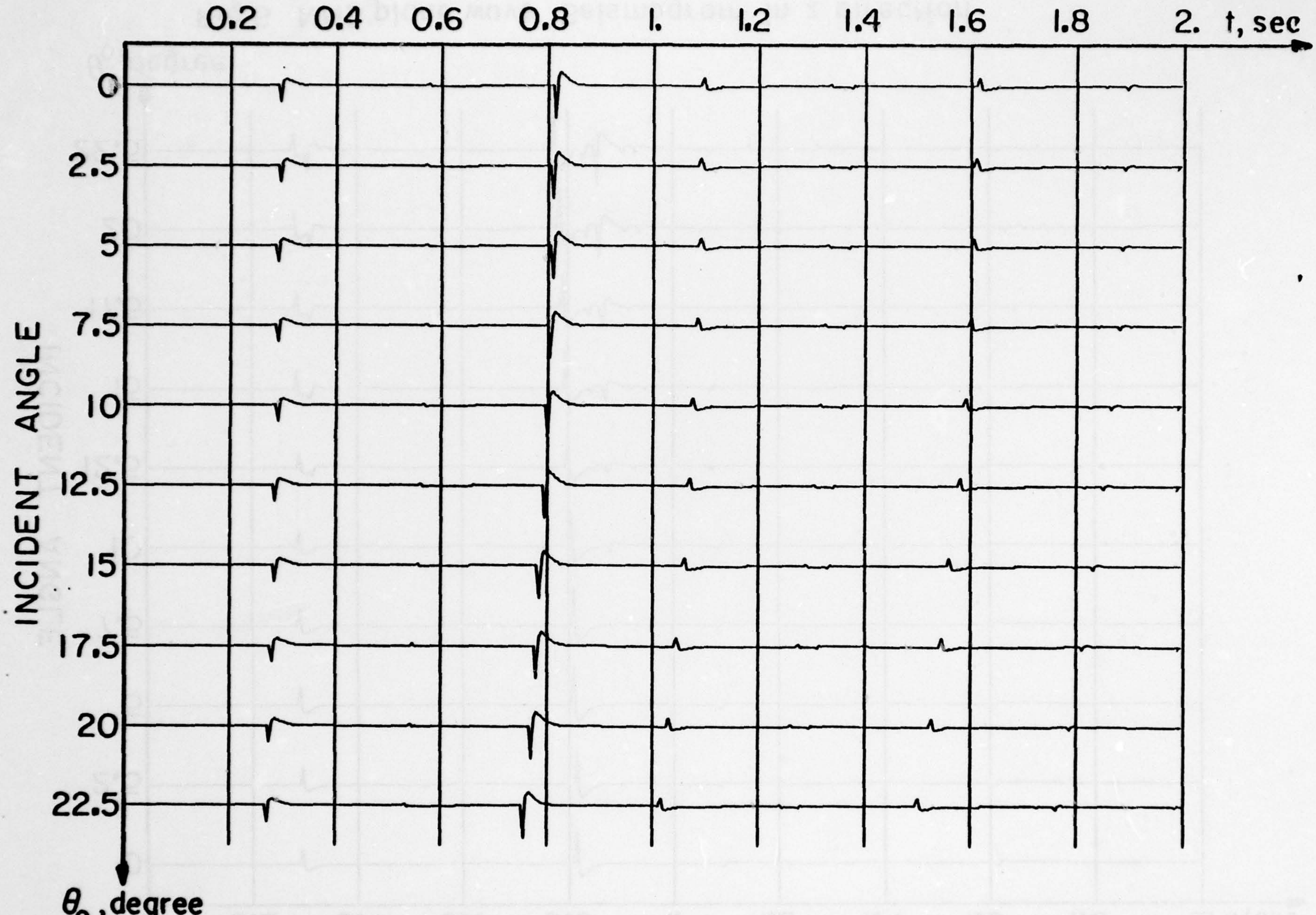

Fig 5 NNI plane wave Seismogram for a 2-layer acoustic model

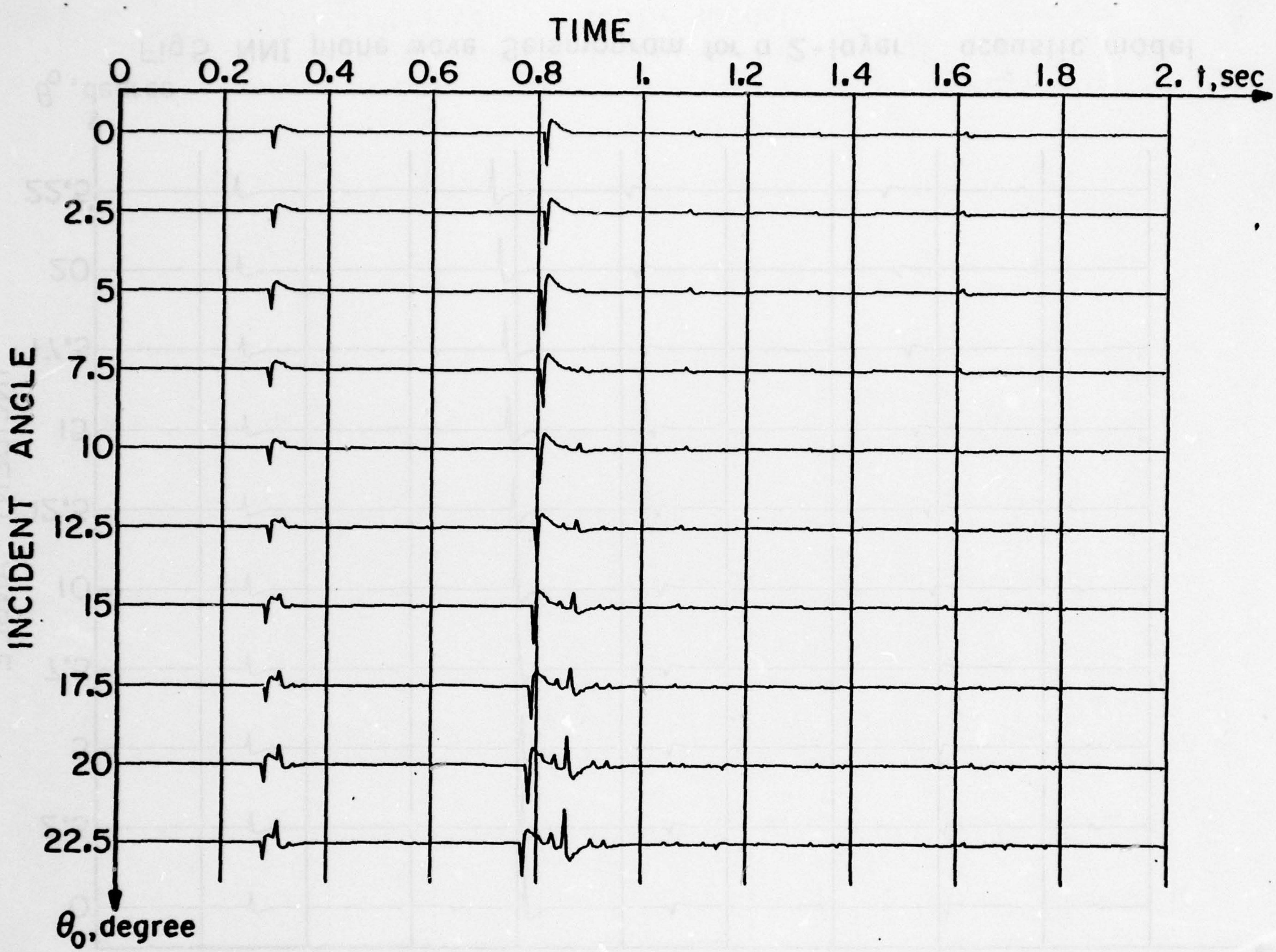

Fig 6 NNI plane wave Seismogram in z direction for a 2-layer elastic model

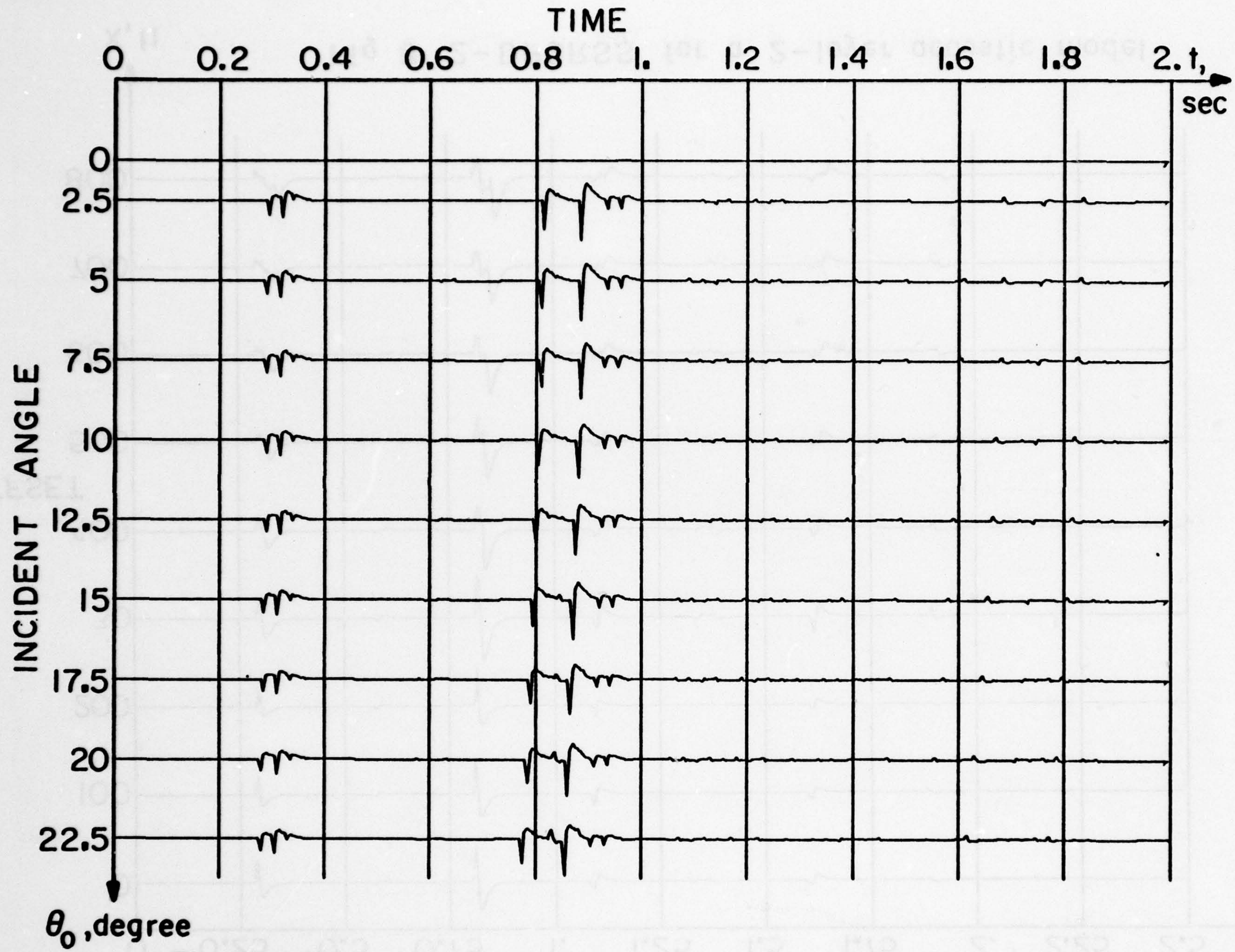

Fig 7 NNI plane wave Seismogram in x direction for a 2-layer elastic model

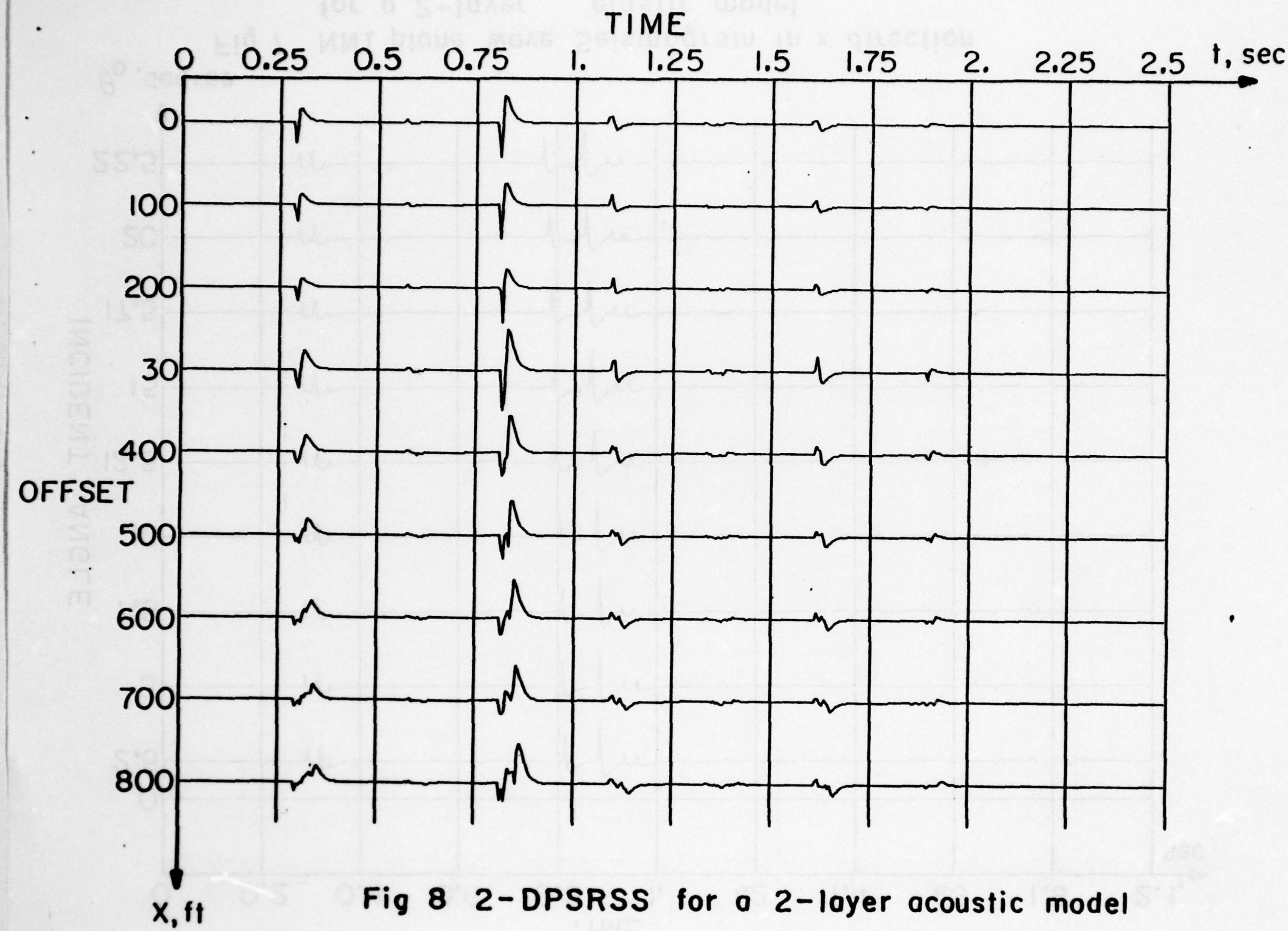

Fig 8 2-DPSRSS for a 2-layer acoustic model

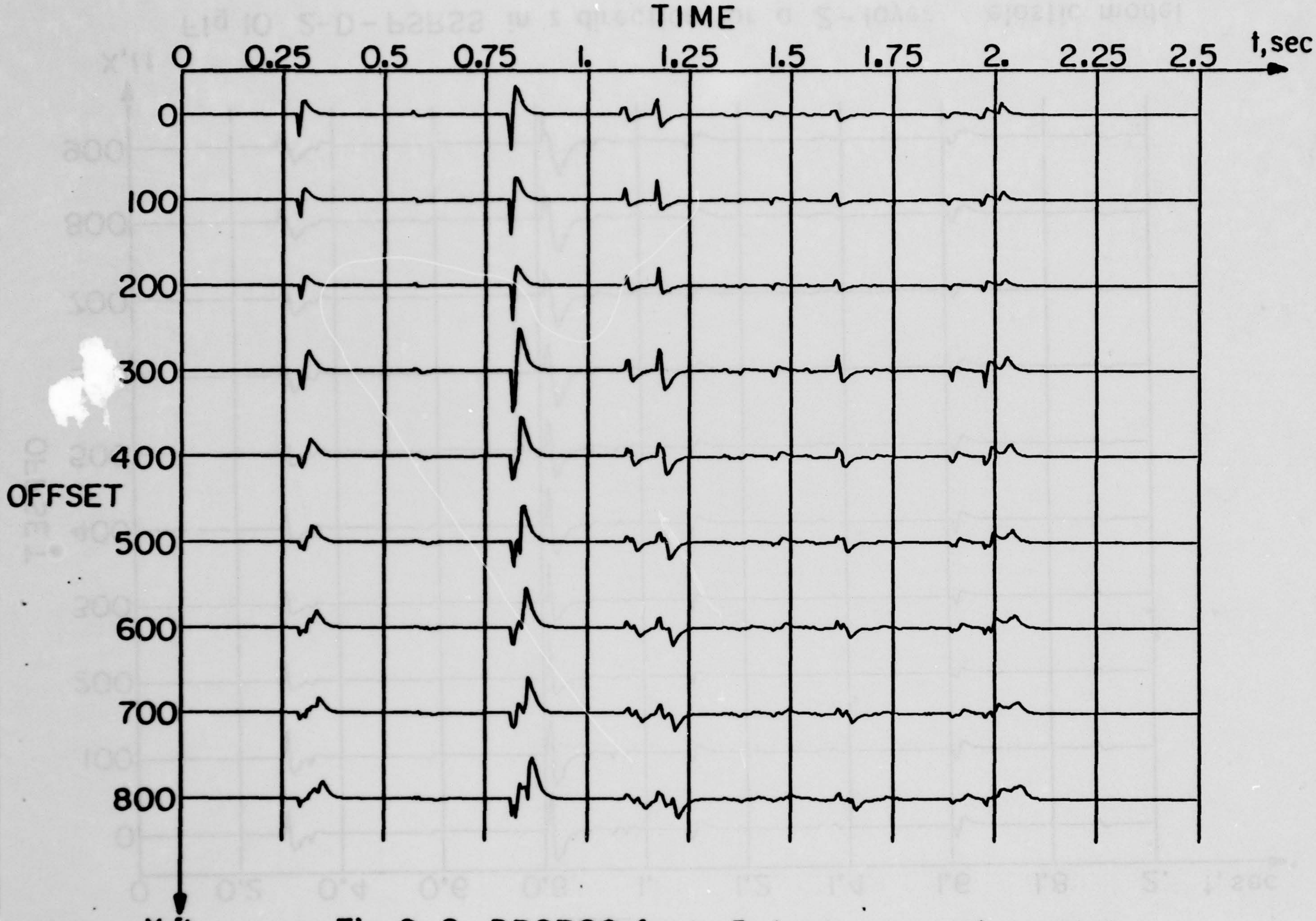

Fig 9 2-DPSRSS for a 3-layer acoustic model

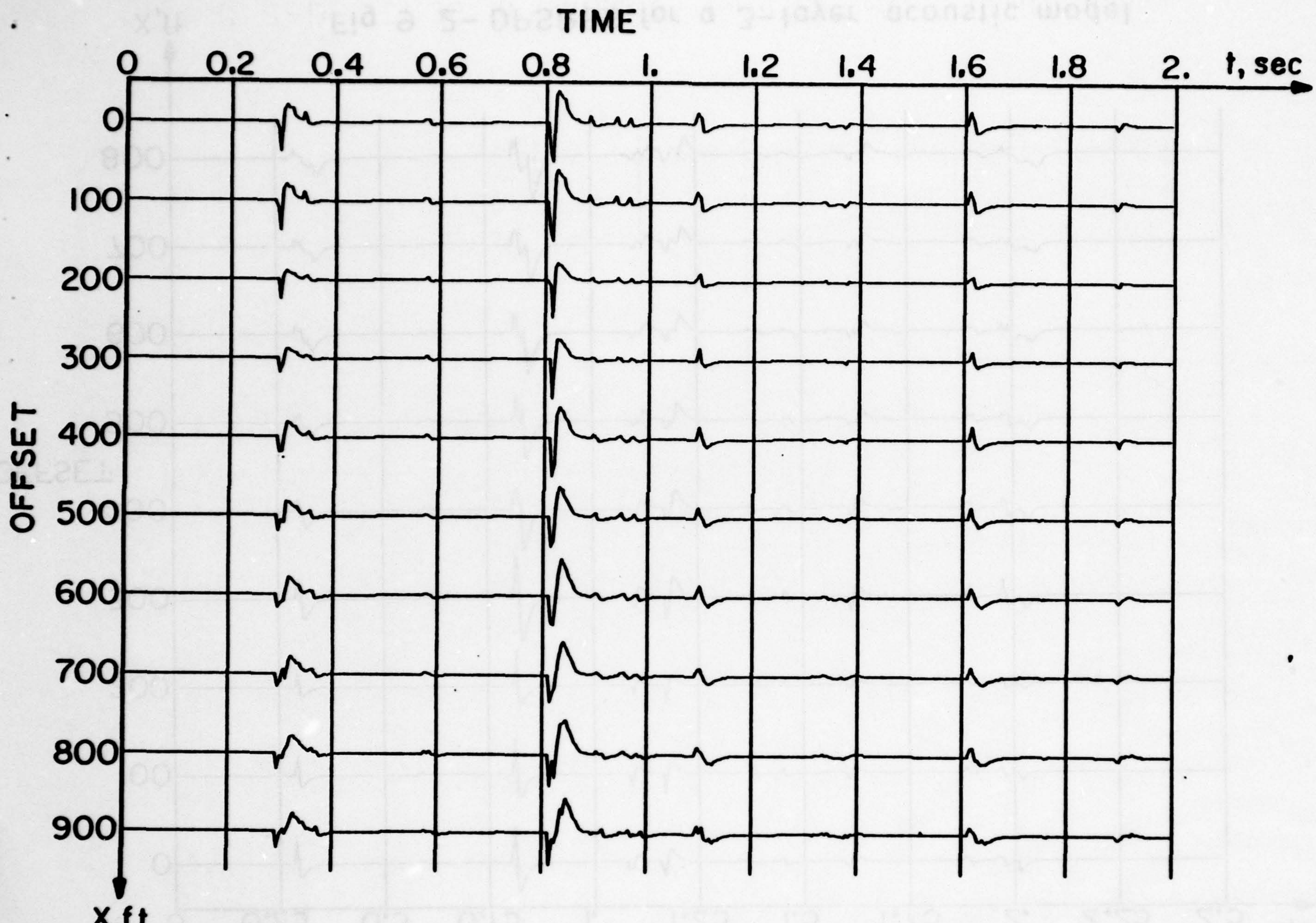

Fig 10 2-D-PSRSS in z direction for a 2-layer elastic model

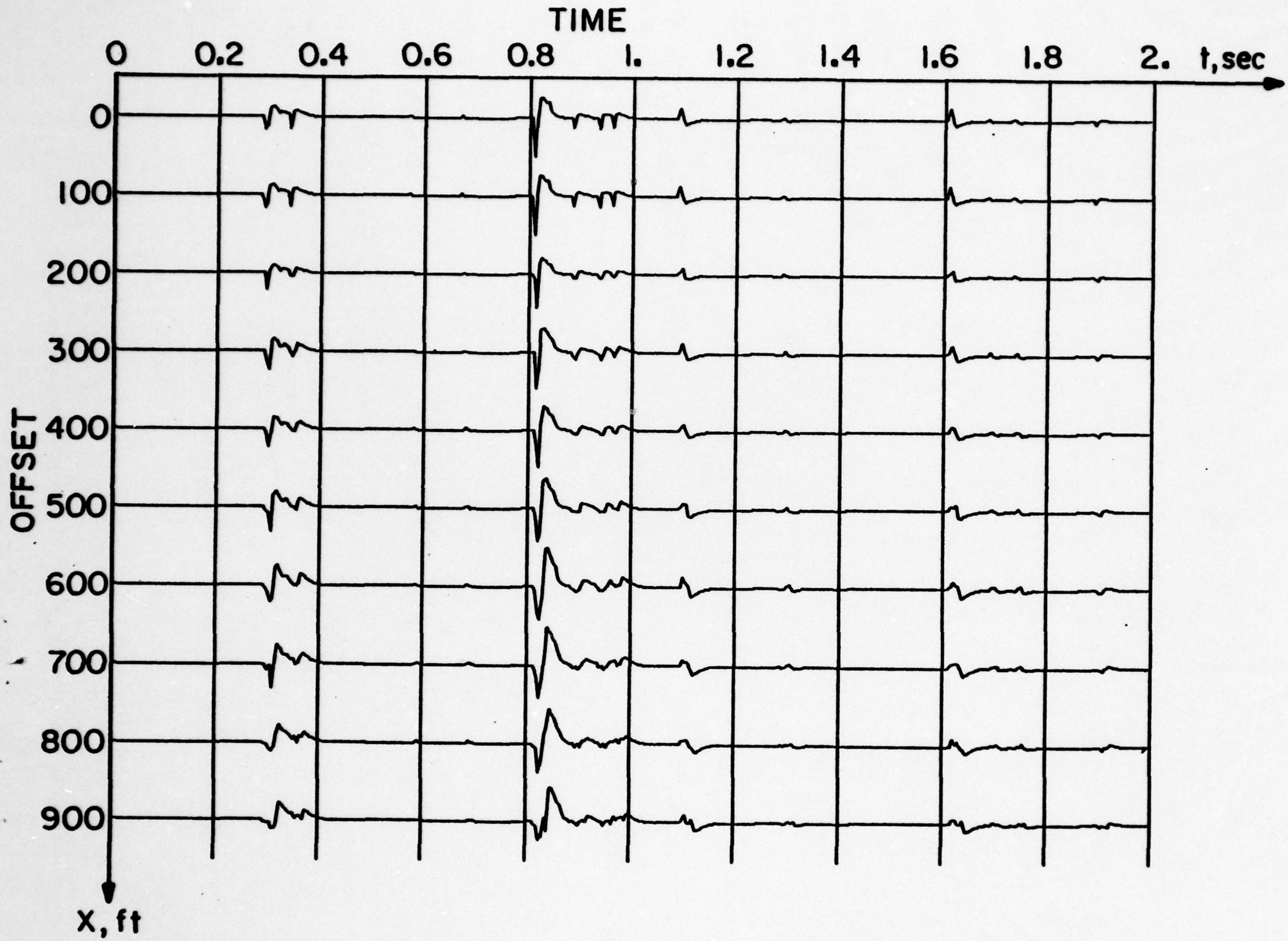

Fig 11 2-D-PSRSS in x direction for a 2-layer elastic model

SECURITY CLASSIFICATION OF THIS PAGE (When Data Entered)

19 REPORT DOCUMENTATION PAGE		READ INSTRUCTIONS BEFORE COMPLETING FORM
1. REPORT NUMBER 18 AFOSR-TR- 79-0048	2. GOVT ACCESSION NO.	3. RECIPIENT'S CATALOG NUMBER
4. TITLE (and Subtitle) 6 NON-NORMAL INCIDENCE STATE SPACE MODEL.		5. TYPE OF REPORT & PERIOD COVERED 9 Interim rept.
		6. PERFORMING ORG. REPORT NUMBER
7. AUTHOR(s) 10 F. Aminzadeh and J.M. Mendel Fereydoun/Aminzadeh Jerry M./Mendel		8. CONTRACT OR GRANT NUMBER(s) 15 AFOSR-75-2797, NSF-ENG74-02297
9. PERFORMING ORGANIZATION NAME AND ADDRESS University of Southern California Department of Electrical Engineering Los Angeles, CA 90007		10. PROGRAM ELEMENT, PROJECT, TASK AREA & WORK UNIT NUMBERS 16 17 A1 61102F 2304/A1
11. CONTROLLING OFFICE NAME AND ADDRESS Air Force Office of Scientific Research/NM Bldg. 410 Bolling Air Force Base, D. C. 20332		12. REPORT DATE 11 1978
		13. NUMBER OF PAGES 33
14. MONITORING AGENCY NAME & ADDRESS(if different from Controlling Office) 12 35p.		15. SECURITY CLASS. (of this report) UNCLASSIFIED
		15a. DECLASSIFICATION/DOWNGRADING SCHEDULE

16. DISTRIBUTION STATEMENT (of this Report)

Approved for public release; distribution unlimited.

17. DISTRIBUTION STATEMENT (of the abstract entered in Block 20, if different from Report)

18. SUPPLEMENTARY NOTES

19. KEY WORDS (Continue on reverse side if necessary and identify by block number)

20. ABSTRACT (Continue on reverse side if necessary and identify by block number)

The primary purpose of this paper is to extend a newly published normal incidence state space model ~~[Ref.1]~~[1] to a non-normal incidence case. It also provides a synthetic seismogram for a two-dimensional point source and different offsets. The non-normal incidence state space model is structurally the same as the normal incidence state space model except that it has twice as many state variables. Because of the mode conversion in non-normal incidence, the scalar upgoing and downgoing waves and travel

DD FORM 1473 1 JAN 73

361 560 UNCLASSIFIED next page

SECURITY CLASSIFICATION OF THIS PAGE (When Data Entered)

20. Abstract continued.

times in each layer as well as reflection and transmission coefficients at each interface are replaced by a vector of upgoing and downgoing waves, a vector of travel time, and matrices of reflection and transmission coefficents respectively. To obtain a two-dimensional point source synthetic seismogram we apply a new version of Sommerfiled's theorem, which is generally used to express a three-dimensional point source in terms of a superposition of line sources.